

Preparation and physical characteristics of solvent intercalated poly(o-ethoxyaniline)/organoclay nanocomposites

J. H. SUNG, J. Y. SHIN, H. J. CHOI

Department of Polymer Science and Engineering, Inha University, Incheon, 402-751, Korea
E-mail: hjchoi@inha.ac.kr

M. S. JHON

Department of Chemical Engineering, Carnegie Mellon University, Pittsburgh, PA 15213-3890, USA

Intercalation of polymers in clay layers has been widely accepted as the most advanced method to synthesize nanophase organic-inorganic hybrids. Here, the clay consists of both anionically charged layers of aluminum/magnesium silicates and small cations such as sodium or potassium located in silicate interlayer galleries [1]. These silicate layers exchange organic cation molecules and swell under certain solvents. Thereby, the polymer solution intercalation method is based on a solvent quality, i.e., whether the polymer is soluble and the silicate layers are swellable [2]. The driving force for polymer intercalation into a layered silicate from solution is the enthalpy gained by desorption of solvent molecules, which compensates for the entropy loss due to the confinement of intercalated chains [3].

Polyaniline (PANI) is one of the best known conducting polymers for commercial applications, because of its environmental stability, good processability, and relatively low cost. However, it contains large equilibrium polyene rings with torsional displacement out of the plane defined by the ring bridging atoms (amine/imine nitrogens). Because of the stiffness, it is very difficult to dissolve the PANI in common organic solvents. However, PANI's derivatives including substituent groups ($-\text{CH}_3$, $-\text{OCH}_3$ or $-\text{OC}_2\text{H}_5$) in monomer or polymeric chain show an excellent solubility in various organic solvents. Despite of its lower conductivity than that of PANI, the poly(o-ethoxyaniline) (PEOA) substituted with $-\text{OC}_2\text{H}_5$ in PANI has attracted much attention due to its good solubility and corrosion resistance in metallic surfaces [4]. The conducting polymer/clay nanocomposite system has also been used not only to enhance the processability (colloidal stability or mechanical strength) [5, 6] but also to improve physical properties. Polypyrrole/montmorillonite (MMT) nanocomposites were synthesized by an emulsion polymerization using dodecylbenzene sulfonic acid [7], and PANI/clay nanocomposites [5, 8, 9] have been reported to improve physical properties including electrical conductivity and electrorheological performance.

In the work reported in this letter, we synthesized soluble PEOA and prepared PEOA/clay nanocomposites. Here, the organic clay was a natural MMT modified with a quaternary ammonium salt of dimethyl, hydrogenated tallow, 2-ethylhexyl quaternary ammonium. Characteristics of PEOA/clay nanocomposites

were investigated for two different compositions of the PEOA. Electrical conductivity can be controlled by the clay contents in the intercalated PEOA/clay nanocomposites.

At first the PEOA, as a soluble conducting polymer in organic solvent, was synthesized. A 0.6 mol ethoxyaniline monomer (Aldrich, USA) in $4 \times 10^{-4} \text{ m}^3$ of 1 M HCl was stirred for 2 h, and the polymerization was initiated at 25 °C by adding a solution of 0.36 mol ammonium persulfate as an oxidizing agent in $2.4 \times 10^{-4} \text{ m}^3$ of 1 M HCl. Products of PEOA (pH = 1) were dried at 25 °C for 2 days using a vacuum oven. The organic clay (OMMT), Cloisite 25A (Southern Clay Product, USA), was swollen in chloroform for 1 day. The PEOA particles were simultaneously dissolved in chloroform. Fixed amounts of clay and PEOA in chloroform solutions were mixed together and stirred for 1 day. This mixed solution was filtered and dried at 25 °C for 2 days using a vacuum oven. The powder form of the products was obtained. Fourier Transform Infrared (FT-IR) spectroscopy (Perkin Elmer System 2000) was used to identify the chemical structure of the PEOA which was prepared as a disk, dispersed in KBr. The intercalation of PEOA/clay nanocomposite was examined via transmission electron microscope (TEM) (CM 200, Philips). The X-ray diffraction (XRD) measurement, using the Rigaku DMAX 2500 ($\lambda = 0.154 \text{ nm}$) diffractometer, was also performed. The conductivity of PEOA particles and nanocomposites was measured with a pressed disk of polymer using a 2-probe method with silver electrodes on each side [7]. The pellets of PEOA particles were prepared using a $1.3 \times 10^{-2} \text{ m}$ KBr pellet die, and the pellet resistance was measured using a picoammeter (Keithley model 487, Cleveland, USA) with a conductivity cell. The conductivity (σ) was then obtained from the following Equation 1,

$$\sigma = d/(A \cdot R)$$

Here d is the thickness (m), A is the surface area (m^2) and R is the resistance of the pellet ($1/S$). σ values are compared by intercalation, adjusting doping and dedoping of PEOA particles.

Fig. 1 shows the FT-IR spectrum of the synthesized PEOA and PEOA/clay nanocomposites. Characteristic

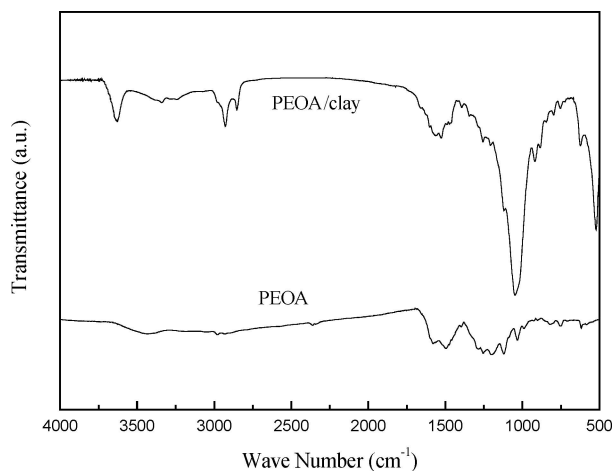


Figure 1 FT-IR spectra of the PEOA and PEOA/clay nanocomposites.

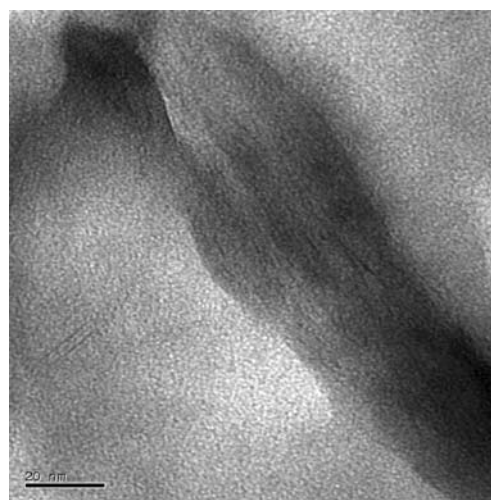
peaks of the PEOA are designated by the aromatic ether at 1000 and 1300 cm^{-1} . In addition, these peaks show the aromatic C—H at 824 cm^{-1} , aromatic amine at 1144 and 1309 cm^{-1} , and aromatic C—C at 1490 and 1586 cm^{-1} . Based on these characteristic peaks from the PEOA, we confirmed nanocomposite formation.

Fig. 2 displays the sectional micrograph of the microtomed nanocomposites obtained from the TEM. The TEM images of PEOA/clay nanocomposites with PEOA components of 25% (a) and 75% (b) show successful intercalation of PEOA into clay gallery layers. In addition, the soluble PEOA particles are well dispersed in clay interlayers. Although these micrographs exhibit the swelling of clay, it is difficult to analyze the extension of interlayer spacing quantitatively.

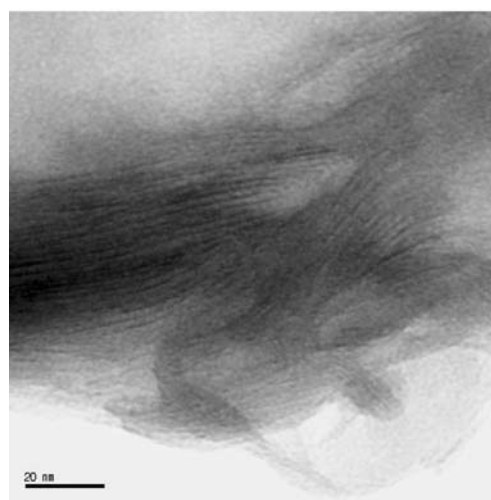
Fig. 3 indicates the XRD pattern for PEOA/clay nanocomposites with different PEOA contents. The peak at $2\theta = 4.8^\circ$ (d -spacing of 1.84 nm from Bragg's law) corresponds to crystallographic planes of the pristine organoclay layer, (001) basal spacing reflection. The d -spacing expansion was identified from the shift of the diffraction peak to lower angles: $2\theta = 4.18^\circ$ (d -spacing of 2.11 nm) for PEOA25/clay and 3.18° for PEOA75/clay (d -spacing of 2.78 nm). These spacings indicate the degree of intercalation of clay with PEOA [10, 11].

Electrical conductivity was calculated from Equation 1 for two different contents of PEOA. Electrical conductivities of pure PEOA, PEOA 25, and PEOA 75 were measured to be 2.0×10^{-2} , 7.3×10^{-8} , and $6.2 \times 10^{-5}\text{ S/m}$, respectively. This effect of particle conductivity was an important factor for the delocalization of charge carriers and weakening the interchain intercalation. The changes of conductivity was attributed to the fact that intercalation into clay takes a role of resistance of the PEOA [12]. The electrical conductivity could be controlled by the intercalation of PEOA contents into the clay interlayers. Thereby, PEOA/clay nanocomposites with relatively low electrical conductivity can be adopted as electrorheological (ER) materials. The ER fluid exhibits reversible changes in its rheological properties as a function of electric field strength [10].

In conclusion, the PEOA was prepared by chemical oxidation polymerization and PEOA/clay nanocomposites were intercalated via a solvent casting process.



(a)



(b)

Figure 2 TEM images of PEOA/clay nanocomposites for two different PEOA contents.(a) 25% and (b) 75%.

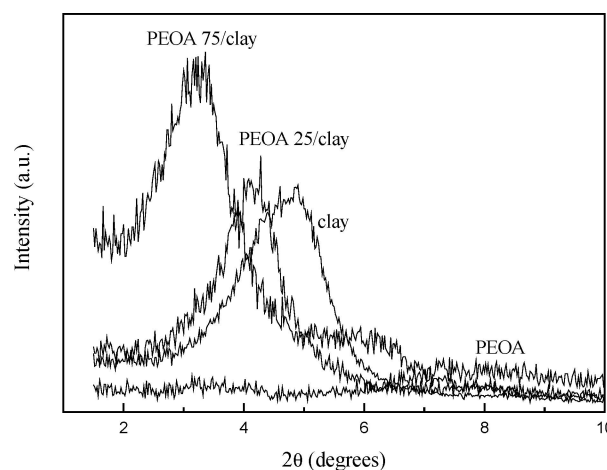


Figure 3 XRD pattern of PEOA, clay, and PEOA/clay nanocomposites.

The d -spacing of PEOA/clay nanocomposites was increased to be 2.11 nm for PEOA25 and 2.78 nm for PEOA75 from the original d -spacing, 1.84 nm of the pristine clay. The PEOA75/clay nanocomposites exhibited larger d -spacing than PEOA25/clay. Electrical conductivity depended on the PEOA intercalation into clay gallery, and became smaller than that of pure PEOA.

Acknowledgement

This study was supported by research grants from the Korea Science and Engineering Foundation through the Applied Rheology Center (ARC) at Korea University, Seoul, Korea

References

1. M. OGAWA and Y. TAKIZAWA, *Chem. Mater.* **11** (1999) 30.
2. J. HEINEMANN, P. REICHERT, R. THOMANN and R. MÜLHAUPT, *Macromol. Rapid Comm.* **20** (1999) 423.
3. R. A. VAIA and E. P. GIANNELIS, *Macromolecules* **30** (1997) 7990.
4. S. V. MELLO, L. H. C. MATTOSO, R. M. FARIA and O. N. OLIVEIRA, *Synth. Met.* **71** (1995) 2039.
5. B. H. KIM, J. H. JUNG, J. JOO, A. J. EPSTEIN, K. MIZOGUCHI, J. W. KIM and H. J. CHOI, *Macromolecules* **35** (2002) 1419.
6. B. H. KIM, J. H. JUNG, J. W. KIM, H. J. CHOI and J. JOO, *Synth. Met.* **121** (2001) 1311.
7. B. H. KIM, S. H. HONG, J. JOO, I. W. PARK, A. J. EPSTEIN, J. W. KIM and H. J. CHOI, *J. Appl. Phys.* **95** (2004) 2697.
8. J. W. KIM, S. G. KIM, H. J. CHOI, M. S. SUH, M. J. SHIN and M. S. JHON, *Int. J. Mod. Phys. B* **15** (2001) 657.
9. J. LU and X. P. ZHAO, *Int. J. Phys. B* **16** (2002) 2521.
10. H. J. CHOI, J. W. KIM, M. S. CHO, S. G. KIM and M. S. JHON, *Eur Polym. J.* **33** (1997) 699.
11. T. H. KIM, L. W. JANG, D. C. LEE, H. J. CHOI and M. S. JHON, *Macromol. Rapid Commun.* **23** (2002) 191.
12. J. M. YEH, *Polymer* **43** (2002) 2729.

Received 11 May
and accepted 8 November 2004